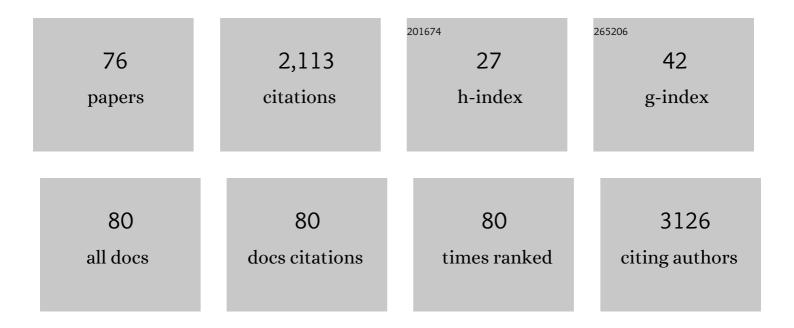
List of Publications by Year in descending order

Source: https://exaly.com/author-pdf/4492801/publications.pdf Version: 2024-02-01



SHILZHANC

#	Article	IF	CITATIONS
1	6:2 and 8:2 Fluorotelomer Alcohol Anaerobic Biotransformation in Digester Sludge from a WWTP under Methanogenic Conditions. Environmental Science & Technology, 2013, 47, 4227-4235.	10.0	118
2	Biotransformation potential of 6:2 fluorotelomer sulfonate (6:2 FTSA) in aerobic and anaerobic sediment. Chemosphere, 2016, 154, 224-230.	8.2	109
3	miRNA-132-3p inhibits osteoblast differentiation by targeting Ep300 in simulated microgravity. Scientific Reports, 2015, 5, 18655.	3.3	81
4	miR-33-5p, a novel mechano-sensitive microRNA promotes osteoblast differentiation by targeting Hmga2. Scientific Reports, 2016, 6, 23170.	3.3	78
5	miR-612 suppresses the stemness of liver cancer via Wnt/β-catenin signaling. Biochemical and Biophysical Research Communications, 2014, 447, 210-215.	2.1	77
6	Effects of Simulated Microgravity on Human Umbilical Vein Endothelial Cell Angiogenesis and Role of the PI3K-Akt-eNOS Signal Pathway. PLoS ONE, 2012, 7, e40365.	2.5	73
7	Role of C/EBP homologous protein and endoplasmic reticulum stress in asthma exacerbation by regulating the IL-4/signal transducer and activator of transcription 6/transcription factor EC/IL-4 receptor I± positive feedback loop in M2 macrophages. Journal of Allergy and Clinical Immunology, 2017, 140, 1550-1561.e8.	2.9	69
8	MicroRNA-139-3p regulates osteoblast differentiation and apoptosis by targeting ELK1 and interacting with long noncoding RNA ODSM. Cell Death and Disease, 2018, 9, 1107.	6.3	64
9	Methodological and physiological variability within the ventilatory response to hypoxia in humans. Journal of Applied Physiology, 2000, 88, 1924-1932.	2.5	57
10	MiR-103 inhibits osteoblast proliferation mainly through suppressing Cav1.2 expression in simulated microgravity. Bone, 2015, 76, 121-128.	2.9	57
11	Impact of 6:2 fluorotelomer alcohol aerobic biotransformation on a sediment microbial community. Science of the Total Environment, 2017, 575, 1361-1368.	8.0	57
12	Simulated weightlessness aggravates hypergravity-induced impairment of learning and memory and neuronal apoptosis in rats. Behavioural Brain Research, 2009, 199, 197-202.	2.2	56
13	Mechanobiological Modulation of Cytoskeleton and Calcium Influx in Osteoblastic Cells by Short-Term Focused Acoustic Radiation Force. PLoS ONE, 2012, 7, e38343.	2.5	53
14	Modeled microgravity causes changes in the cytoskeleton and focal adhesions, and decreases in migration in malignant human MCF-7 cells. Protoplasma, 2009, 238, 23-33.	2.1	47
15	Insights on N-glycosylation of human haptoglobin and its association with cancers. Glycobiology, 2016, 26, 684-692.	2.5	47
16	MiRâ€103â€3p targets the m ⁶ A methyltransferase METTL14 to inhibit osteoblastic bone formation. Aging Cell, 2021, 20, e13298.	6.7	47
17	Effects of N-acetylcysteine and glutathione ethyl ester drops on streptozotocin-induced diabetic cataract in rats. Molecular Vision, 2008, 14, 862-70.	1.1	41
18	Hyperbaric oxygen preconditioning reduces ischemia–reperfusion injury by stimulating autophagy in neurocyte. Brain Research, 2010, 1323, 149-151.	2.2	39

#	Article	IF	CITATIONS
19	Simulated microgravity inhibits L-type calcium channel currents partially by the up-regulation of miR-103 in MC3T3-E1 osteoblasts. Scientific Reports, 2015, 5, 8077.	3.3	39
20	Oct4 induces EMT through LEF1/β-catenin dependent WNT signaling pathway in hepatocellular carcinoma. Oncology Letters, 2017, 13, 2599-2606.	1.8	39
21	TMCO1-mediated Ca2+ leak underlies osteoblast functions via CaMKII signaling. Nature Communications, 2019, 10, 1589.	12.8	38
22	MiR-30 family members inhibit osteoblast differentiation by suppressing Runx2 under unloading conditions in MC3T3-E1 cells. Biochemical and Biophysical Research Communications, 2020, 522, 164-170.	2.1	37
23	Online solid sampling platform using multi-wall carbon nanotube assisted matrix solid phase dispersion for mercury speciation in fish by HPLC-ICP-MS. Journal of Analytical Atomic Spectrometry, 2015, 30, 882-887.	3.0	34
24	Focal adhesion kinase signaling pathway is involved in mechanotransduction in MG-63 Cells. Biochemical and Biophysical Research Communications, 2011, 410, 671-676.	2.1	33
25	Treatment of chronic subdural hematoma with atorvastatin combined with low-dose dexamethasone: phase II randomized proof-of-concept clinical trial. Journal of Neurosurgery, 2021, 134, 235-243.	1.6	33
26	Ethylene/propylene copolymerization catalyzed by vanadium complexes containing N-heterocyclic carbenes. Dalton Transactions, 2015, 44, 15264-15270.	3.3	32
27	Serum fucosylated paraoxonase 1 as a potential glycobiomarker for clinical diagnosis of early hepatocellular carcinoma using ELISA Index. Glycoconjugate Journal, 2015, 32, 119-125.	2.7	30
28	Quantitative analysis of site-specific <italic>N</italic> -glycans on sera haptoglobin β chain in liver diseases. Acta Biochimica Et Biophysica Sinica, 2013, 45, 1021-1029.	2.0	28
29	Targeted silencing of miRNA-132-3p expression rescues disuse osteopenia by promoting mesenchymal stem cell osteogenic differentiation and osteogenesis in mice. Stem Cell Research and Therapy, 2020, 11, 58.	5.5	28
30	iTRAQ plus 180: A new technique for target glycoprotein analysis. Talanta, 2012, 91, 122-127.	5.5	27
31	Targeted overexpression of the long noncoding RNA ODSM can regulate osteoblast function in vitro and in vivo. Cell Death and Disease, 2020, 11, 133.	6.3	27
32	Osteoblast-targeted delivery of miR-33-5p attenuates osteopenia development induced by mechanical unloading in mice. Cell Death and Disease, 2018, 9, 170.	6.3	26
33	Simulated Microgravity Promotes Angiogenesis through RhoA-Dependent Rearrangement of the Actin Cytoskeleton. Cellular Physiology and Biochemistry, 2017, 41, 227-238.	1.6	25
34	Bone-targeted lncRNA OGRU alleviates unloading-induced bone loss via miR-320-3p/Hoxa10 axis. Cell Death and Disease, 2020, 11, 382.	6.3	25
35	Aided Diagnosis of Hepatocellular Carcinoma Using Serum Fucosylated Haptoglobin Ratios. Journal of Cancer, 2017, 8, 887-893.	2.5	23
36	Simulated microgravity reduces intracellularâ€free calcium concentration by inhibiting calcium channels in primary mouse osteoblasts. Journal of Cellular Biochemistry, 2019, 120, 4009-4020.	2.6	22

#	Article	IF	CITATIONS
37	Diagnosis of AFP-negative early-stage hepatocellular carcinoma using Fuc-PON1. Discovery Medicine, 2017, 23, 163-168.	0.5	22
38	Clinorotation upregulates inducible nitric oxide synthase by inhibiting APâ€1 activation in human umbilical vein endothelial cells. Journal of Cellular Biochemistry, 2009, 107, 357-363.	2.6	21
39	The Impact of Simulated Weightlessness on Endothelium-Dependent Angiogenesis and the Role of Caveolae/Caveolin-1. Cellular Physiology and Biochemistry, 2016, 38, 502-513.	1.6	21
40	CircRNA_0050463 promotes influenza A virus replication by sponging miR-33b-5p to regulate EEF1A1. Veterinary Microbiology, 2021, 254, 108995.	1.9	21
41	GP73 N-glycosylation at Asn144 reduces hepatocellular carcinoma cell motility and invasiveness. Oncotarget, 2016, 7, 23530-23541.	1.8	20
42	Quantification of N-glycosylation site occupancy status based on labeling/label-free strategies with LC-MS/MS. Talanta, 2017, 170, 509-513.	5.5	19
43	Influence of Rib Structure and Elastic Yarn Type Variations on Textile Piezoresistive Strain Sensor Characteristics. Fibres and Textiles in Eastern Europe, 2018, 26, 24-31.	0.5	19
44	Targeting CDC7 potentiates ATR-CHK1 signaling inhibition through induction of DNA replication stress in liver cancer. Genome Medicine, 2021, 13, 166.	8.2	19
45	Multiple lectin assays for detecting glyco-alteration of serum GP73 in liver diseases. Glycoconjugate Journal, 2015, 32, 657-664.	2.7	17
46	The impact of extraversion on attentional bias to pleasant stimuli: neuroticism matters. Experimental Brain Research, 2016, 234, 721-731.	1.5	17
47	Clinorotation enhances autophagy in vascular endothelial cells. Biochemistry and Cell Biology, 2013, 91, 309-314.	2.0	16
48	Aberrant expression of Golgi protein 73 is indicative of a poor outcome in hepatocellular carcinoma. Oncology Reports, 2016, 35, 2141-2150.	2.6	16
49	Reversal of the Detrimental Effects of Simulated MicrogravityÂon Human Osteoblasts by Modified Low IntensityÂPulsed Ultrasound. Ultrasound in Medicine and Biology, 2013, 39, 804-812.	1.5	15
50	Assessment of Hepatocellular Carcinoma Metastasis Glycobiomarkers Using Advanced Quantitative N-glycoproteome Analysis. Frontiers in Physiology, 2017, 8, 472.	2.8	15
51	miRâ€181câ€5p mediates simulated microgravityâ€induced impaired osteoblast proliferation by promoting cell cycle arrested in the G 2 phase. Journal of Cellular and Molecular Medicine, 2019, 23, 3302-3316.	3.6	14
52	Discovering potential serological biomarker for chronic Hepatitis B Virus-related hepatocellular carcinoma in Chinese population by MAL-associated serum glycoproteomics analysis. Scientific Reports, 2017, 7, 38918.	3.3	12
53	21-day Balneotherapy Improves Cardiopulmonary Function and Physical Capacity of Pilots. Journal of Physical Therapy Science, 2013, 25, 109-112.	0.6	11
54	Acceleration after-effects on learning and memory in rats: +10Gz or +6Gz for 3min. Neuroscience Letters, 2007, 413, 245-248.	2.1	10

#	Article	IF	CITATIONS
55	Effect of 3 Weeks of Balneotherapy on Immunological Parameters, Trace Metal Elements and Mood States in Pilots. Journal of Physical Therapy Science, 2013, 25, 51-54.	0.6	10
56	Genome-wide analysis and prediction of functional long noncoding RNAs in osteoblast differentiation under simulated microgravity. Molecular Medicine Reports, 2017, 16, 8180-8188.	2.4	10
57	Effect of a 21-day balneotherapy program on blood cell counts, ponogen levels, and blood biochemical indexes in servicemen in sub-health condition. Journal of Physical Therapy Science, 2017, 29, 1573-1577.	0.6	10
58	HSF1 promotes the inhibition of EMT-associated migration by low glucose via directly regulating Snail1 expression in HCC cells. Discovery Medicine, 2016, 22, 87-96.	0.5	9
59	Lower body negative pressure protects brain perfusion in aviation gravitational stress induced by push–pull manoeuvre. Journal of Physiology, 2020, 598, 3173-3186.	2.9	7
60	Circulating Exosomes from Mice with LPS-Induced Bone Loss Inhibit Osteoblast Differentiation. Calcified Tissue International, 2022, 111, 185-195.	3.1	6
61	The combined effects of simulated microgravity and X-ray radiation on MC3T3-E1 cells and rat femurs. Npj Microgravity, 2021, 7, 3.	3.7	4
62	Integration and application of 3D visualization technology and numerical simulation technology in geological research. Environmental Earth Sciences, 2021, 80, 1.	2.7	4
63	Rapid diagnosis of hepatocellular carcinoma using a haptoglobin ELISA assay based on AAL-coated magnetic beads. Discovery Medicine, 2016, 22, 97-104.	0.5	4
64	Identification and characterization of circular RNAs in the A549 cells following Influenza A virus infection. Veterinary Microbiology, 2022, 267, 109390.	1.9	4
65	Atorvastatin combined with dexamethasone in chronic subdural haematoma (ATOCH II): study protocol for a randomized controlled trial. Trials, 2021, 22, 905.	1.6	4
66	The small protein MafG plays a critical role in MC3T3-E1 cell apoptosis induced by simulated microgravity and radiation. Biochemical and Biophysical Research Communications, 2021, 555, 175-181.	2.1	3
67	HDAC6 Negatively Regulates miR-155-5p Expression to Elicit Proliferation by Targeting RHEB in Microvascular Endothelial Cells under Mechanical Unloading. International Journal of Molecular Sciences, 2021, 22, 10527.	4.1	3
68	A Protective Role of Tumor Necrosis Factor Superfamily-15 in Intracerebral Hemorrhage-Induced Secondary Brain Injury. ASN Neuro, 2021, 13, 175909142110384.	2.7	3
69	Insight Into an Outbreak of Canine Distemper Virus Infection in Masked Palm Civets in China. Frontiers in Veterinary Science, 2021, 8, 728238.	2.2	3
70	ELISA index of serum fucosylated haptoglobin for diagnosis of HCC using the normal and reverse AAL ELISA. Discovery Medicine, 2016, 21, 15-23.	0.5	3
71	The influence of fluid shear stress on the expression of Cbfa1 in MG-63 cells cultured under different gravitational conditions. Advances in Space Research, 2008, 42, 1980-1985.	2.6	2
72	IMAGE IMPROVEMENT IN THE WAVELET DOMAIN FOR OPTICAL COHERENCE TOMOGRAMS. Journal of Innovative Optical Health Sciences, 2011, 04, 73-78.	1.0	2

#	Article	IF	CITATIONS
73	From spindle to spherical: Is spherical shape a potential predictor of human mesenchymal stem cells with increased differentiation capability?. Bioscience Hypotheses, 2009, 2, 407-409.	0.2	1
74	DNA stretching on super-aligned carbon nanotube films. , 2010, , .		0
75	Cuff-Method Thigh Arterial Occlusion Counteracts Cerebral Hypoperfusion Against the Push–Pull Effect in Humans. Frontiers in Physiology, 2021, 12, 672351.	2.8	Ο
76	Systems specificity in responsiveness to intermittent artificial gravity during simulated microgravity in rats. Acta Physiologica Sinica, 2016, 68, 391-402.	0.5	0